

See discussions, stats, and author profiles for this publication at: <https://www.researchgate.net/publication/229010829>

Sol–Gel–Derived Carbon Aerogels and Xerogels: Design of Experiments Approach to Materials Synthesis

ARTICLE *in* INDUSTRIAL & ENGINEERING CHEMISTRY RESEARCH · JUNE 2002

Impact Factor: 2.59 · DOI: 10.1021/ie020048g

CITATIONS

39

READS

58

3 AUTHORS, INCLUDING:



[Shaheen Abdulhafez Al-Muhtaseb](#)

Qatar University

60 PUBLICATIONS 769 CITATIONS

SEE PROFILE

Sol–Gel-Derived Carbon Aerogels and Xerogels: Design of Experiments Approach to Materials Synthesis

Emily J. Zanto, Shaheen A. Al-Muhtaseb, and James A. Ritter*

Department of Chemical Engineering, Swearingen Engineering Center, University of South Carolina, Columbia, South Carolina 29208

A design of experiments approach was conducted to determine the effects of the gel pH (5.5 and 7.0), weight percentage of solids (5 and 20%), pyrolysis temperature (800 and 1050 °C), and gel type (aerogel or xerogel) on the surface area, pore volume, and electrochemical double-layer capacitance of carbonized resorcinol/formaldehyde resins. The full 2^4 factorial design carried out on 16 different materials (8 carbon aerogels and 8 carbon xerogels) and the full 2^3 factorial designs carried out on the carbon aerogels and carbon xerogels individually revealed significant differences between these two types of gels, with specific two-factor interactions observed that could not have been easily resolved with the traditional approach of changing one variable at a time. The gel pH was found to be the most dominant factor (parameter) affecting not only the surface area and pore volumes of both types of gels but also the capacitance, more so for the carbon aerogels in all cases. On average, the carbon aerogels exhibited higher surface areas, pore volumes, and capacitances than the carbon xerogels; in general, higher surface areas correlated with higher pore volumes, and higher capacitances correlated with higher surface areas and also with higher pore volumes, but not as closely. The properties of the carbon aerogels were also more sensitive to the synthesis and processing conditions than those of the carbon xerogels, indicating a broader range of applications for the former but more controllability of synthesis and processing for the latter, and vice versa.

Introduction

Organic aerogels synthesized by the polycondensation of resorcinol with formaldehyde through a reaction mechanism similar to the sol–gel processing of silica and dried supercritically with CO_2 were first introduced by Pekala.¹ Since then, numerous articles have been published on the properties and potential uses not only of these novel “organic” aerogels,^{2–11} but also of pyrolyzed (carbonized) versions referred to as “carbon” aerogels⁵ and even organic and carbon xerogel versions^{12–14} of these highly porous materials. Overall, there has been a noticeable interest in such materials as electrodes for supercapacitors and various types of secondary batteries, as well as for capacitive deionization and other electrosorptive water purification processes.

In general, an aerogel is produced when the solvent contained within the voids of a gelatinous structure is exchanged with an alternative solvent, such as liquid CO_2 , that can be removed supercritically in the absence of a vapor–liquid interface and thus without any interfacial tension. Ideally, this supercritical drying process leaves the gel structure unchanged with no shrinkage of the internal voids or pores.¹⁵ In contrast, a xerogel is produced when the solvent is removed by conventional methods such as evaporation under normal, nonsupercritical conditions. This typical drying process causes the internal gel structure to collapse because of the tremendous interfacial tension caused by the presence of the vapor–liquid interface, especially in the very small voids or pores.¹⁵ It is noteworthy that some authors have referred to their materials as aerogels even though they were actually xerogels because

they were dried conventionally, not supercritically.^{6,16–18} The point here is not terminology, which can be readily clarified based on the experimental procedure. The point is that the physical and chemical properties of organic or carbon aerogels and xerogels are expected to be different. However, none of the aforementioned studies have addressed this very important issue.

Therefore, one of the objectives of this study is to illuminate the differences between carbon aerogels and xerogels using a statistical design of experiments approach. To illustrate the methodology, three other factors (parameters) are also investigated: the initial solution (gel) pH, the weight percent of solids, and the pyrolysis temperature. The response variables studied in this work include the surface area, pore volume, and electrochemical double-layer capacitance. Although these response variables have been studied by Ritter and co-workers in their previous works,^{12–14} their experiments were based on the typical approach of changing one factor at a time, which does not allow for factor interactions to be investigated adequately. In contrast, this study shows how to determine readily not only how each factor affects the response variable of interest, but also how each factor might interact with one another.

Experimental Section

Resorcinol (ACS, >99%, Alfa Aesar), formaldehyde (37% in water, Aldrich), sodium carbonate (anhydrous, ACS, Fisher), nitric acid (HNO_3 , 70.4%, Mallinckrodt), and acetone (optima, 99.6%, Fisher) were used as received. The synthesis procedure for these gels was developed based on the published procedures for making carbon aerogels³ and xerogels.¹² The solutions prepared contained either 5 or 20 wt % solids (on a weight per volume basis), with the R/F (resorcinol/formaldehyde)

* Corresponding author. E-mail: ritter@enr.sc.edu. Tel.: (803) 777-3590. Fax: (803) 777-8265.

mole ratio fixed at 1:2. Sodium carbonate was used as the catalyst, with the R/C (resorcinol/sodium carbonate) mole ratio fixed at 50:1.

Four 1-L batches of "wet" gel were prepared in a glovebox under nitrogen atmosphere using doubly distilled water. These four batches included one with a low initial solution (gel) pH and low weight percentage of solids, one with a high gel pH and low weight percentage of solids, one with a low gel pH and high weight percentage of solids, and one with a high gel pH and high weight percentage of solids. The low and high gel pH values were fixed at 5.5 and 7.0, respectively, by adjusting the solutions with dilute HNO₃. These solutions were then poured into 100-mL glass containers, tightly sealed with caps and stirred magnetically for 30 min. The sealed containers were then removed from the glovebox and placed in an oven at 87 ± 3 °C (without stirring) for 1 week for the solution to gel and cure.

When removed from the oven and cooled to room temperature, each batch was divided into two equal parts. The first part, designated to be xerogel, was washed with acetone for 3 days, with the acetone being replaced daily under vacuum filtration, and then dried in a tube furnace under nitrogen flow. This drying procedure included heating the gel to 65 °C at a heating rate of 5 °C/min, holding it there for 5 h, heating it to 110 °C at a heating rate of 5 °C/min, holding it there for 3 h, and then letting it cool gradually to room temperature. The second part, designated to be aerogel, was broken into medium-sized chunks. These chunks were placed in a dish of acetone inside a vacuum desiccator. The desiccator bottom was filled with Drierite and acetone. A dish of anhydrous Na₂CO₃ was placed in the desiccator on the shelf. The desiccator was evacuated until the acetone began to boil, at which time the desiccator was sealed to maintain the vacuum pressure. The desiccator was opened daily to replace the acetone in which the gel was sitting with fresh acetone and to exchange the saturated Na₂CO₃ with dry Na₂CO₃. This procedure was followed for 1 week to ensure that all of the water in the gel was replaced with acetone.

The acetone-exchanged gel was then transferred into a Polaron supercritical dryer set at 10 °C, which was subsequently filled with liquid CO₂ (Coleman Grade from National Welders Specialty Gases). The gel remained in the CO₂ for 24 h, with the CO₂ being replenished as needed to maintain the liquid level above the gel. In this way, the acetone in the gel was replaced with liquid CO₂. After 24 h of soaking, the temperature of the supercritical dryer was increased until the liquid CO₂ became supercritical (~38 °C). The CO₂ was then released slowly to prevent disruption of the gel structure. Once the pressure was released, the gels were removed from the drier and placed in the nitrogen glovebox until they were pyrolyzed.

The dried organic xerogel and aerogel resins were again separated into two equal parts. One-half was pyrolyzed at 800 °C and the other half at 1050 °C in a tube furnace for 3 h under a 1 L/min nitrogen flow at a heating rate of 5 °C/min. After the 3-h period, the carbonized resins were allowed to cool to room temperature while still under the nitrogen flow. In this way, the initial four batches of wet gel produced 16 different carbonized materials, 8 different carbon aerogels and 8 different carbon xerogels.

A Micromeritics Pulse Chemisorb-2700 analyzer was used to obtain the surface areas and pore volumes of

both the carbon xerogels and aerogels. A single-point BET method was used to obtain the surface areas using 30 vol % N₂ in He (National Welders). The resulting surface areas were calculated from¹⁹

$$S = AN \left(1 - \frac{P}{P_0} \right) \frac{V_a}{M} \quad (1)$$

where V_a is the volume (at STP) of gas adsorbed at a N₂ partial pressure of P (30% of atmospheric pressure), P_0 is the saturation pressure of N₂, A is Avogadro's number (6.023×10^{23} molecules/g-mol), M is the molar volume of the gas (22414 cm³/g-mol at STP), and N is the area of each adsorbed N₂ molecule (estimated as¹⁹ 16.2 Å²). A single-point method was also used to obtain the total pore volumes using 98 vol % N₂ in He (from National Welders) to fill the pores. The resulting pore volumes were calculated from¹⁹

$$V_p = \left(\frac{M_l}{M} \right) V_a \quad (2)$$

where M_l is the molar volume of liquid N₂ (34.670 cm³/g-mol) and M and V_a are as defined above (at STP).

A three-electrode test system was used to measure the single-electrode electrochemical double-layer capacitance. The working electrode, containing 1–2 mg of active material (i.e., the carbonized gel powder) and 5 wt % Teflon as a binder, was hand-pressed into a disk with a diameter of about 0.75 cm and a thickness of about 50 μm. The disk was then pressed between two pieces of platinum gauze at 3 ton/cm² with a hydraulic press and held there for 10 min. A saturated calomel electrode (SCE) was used as the reference electrode, a piece of platinum gauze as the counter electrode, and a solution of 6 M KOH as the electrolyte. The pellet was regenerated at 150 °C for 1 h and soaked in 6 M KOH overnight before being tested. An EG&G model 273A potentiostat was used to run constant current charge and discharge tests on the single carbon electrodes at ambient temperature (25 °C). From these tests, the single-electrode capacitance was calculated from the slope of the voltage response with time using the equation

$$C = \frac{i}{m} \left(\frac{\Delta t}{\Delta V} \right) \quad (3)$$

where i is the current, t is the time, V is the voltage, and m is the mass of the carbon pellet. For these tests, a constant current of 1 mA was used.

Results and Discussion

A full factorial design is an experimental arrangement in which a small integral number of levels, I , is chosen for each of the k factors, and all I^k combinations of these levels are carried out experimentally. In this study, an I value of 2 was chosen for simplicity, as it restricts the design to high and low values of the factors only. These two levels of the four factors (i.e., gel pH, weight percentage of solids, pyrolysis temperature, and gel type) created a full 2⁴ factorial design. These four factors and their high and low levels are given in Table 1. It is noteworthy that these particular factors were selected because they all have been shown to have significant effects on the final properties of the carbon material.^{8,12–14,20}

Table 1. Factors and Factor Settings for the Full 2⁴ Factorial Design

| factor | high setting | low setting |
|--------------------------------|--------------|-------------|
| (A) initial solution (gel) pH | 7.0 | 5.5 |
| (B) weight of solids (%) | 20 | 5 |
| (C) pyrolysis temperature (°C) | 1050 | 800 |
| (D) gel type | aerogel | xerogel |

The three response variables of interest to this study were the surface area, pore volume, and electrochemical double-layer capacitance (single-electrode). The results from the total surface area, pore volume, and capacitance tests for the 2⁴ factorial design are shown in Table 2, along with their averages and standard deviations. The wide standard deviations around the averages show the high potential of these carbon gels, in general, to be tailored to specific applications. It was also of interest to explore the effects of only three of the factors (i.e., gel pH, weight percentage of solids, and pyrolysis temperature) on the properties of the carbon aerogels and xerogels individually. This was accomplished by dividing the full 2⁴ factorial design into two full 2³ factorial designs, one for the carbon aerogels and one for the carbon xerogels. The results from the surface area, pore volume, and capacitance tests for the 2³ factorial designs, as well as the averages and standard deviations from these response variables, are tabulated in Tables 3 and 4 for the carbon aerogels and xerogels, respectively. It is interesting that the averages and standard deviations of the response variables for the carbon aerogels are much wider than those for the carbon xerogels. This indicates not only that the carbon aerogels are more amenable to tailoring, but also that the carbon xerogels are less susceptible to property variation resulting from minor variations in the synthesis and processing conditions, and vice versa.

These response variables were analyzed individually using Taguchi's statistical design method, which is explained in detail elsewhere.²¹ This included completing a response table; calculating the effect of each factor and each factor interaction combination; plotting the effects on Pareto and probability plots; and then, from these plots, determining which effects were significant according to a set fractional confidence limit (1 - α) or comparative analyses.

Surface Area and Pore Volume Analyses. Figure 1 shows the Pareto and normal probability (also called

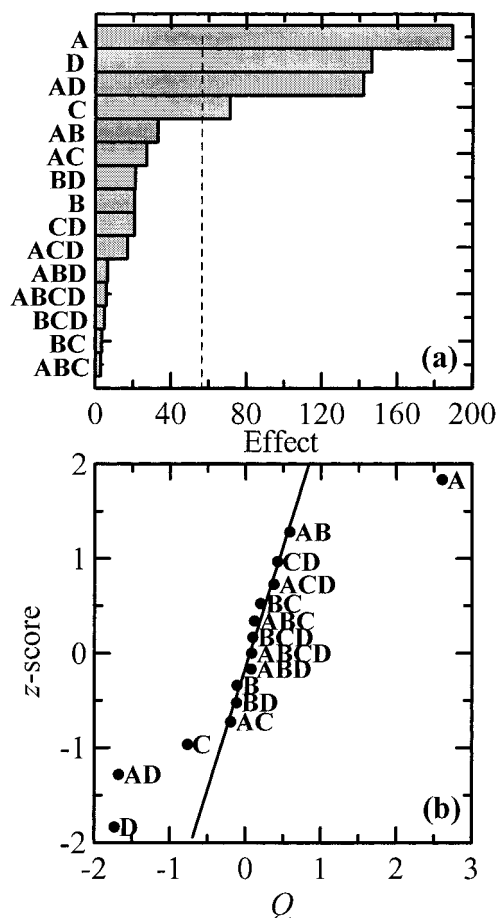


Figure 1. (a) Pareto and (b) normal probability plots for the effects of (A) gel pH, (B) weight percentage of solids, (C) pyrolysis temperature, and (D) gel type on the surface area of the carbon gels. The vertical line in the Pareto plot indicates a confidence limit of 90% ($\alpha = 0.10$).

$Q-Q$ plots for surface area, where Q is the standardized value of the corresponding effect and denotes the ratio of the deviation between the effect and the mean of the effects to the standard deviation of the effects. The z score is an indicator of the cumulative probability of the normal distribution. The Pareto plot (Figure 1a) shows the relative magnitudes of the effects from the 15 combinations corresponding to the effect of each of the

Table 2. Response Variables from the Full 2⁴ Factorial Design

| initial solution pH | solids content (wt %) | pyrolysis temperature (°C) | gel type | surface area (m ² /g) | pore volume (cm ³ /g) | electrochemical capacitance (F/g) |
|----------------------|-----------------------|----------------------------|----------|----------------------------------|----------------------------------|-----------------------------------|
| 5.5 | 5 | 800 | aerogel | 561 | 0.32 | 128 |
| 5.5 | 5 | 800 | xerogel | 569 | 0.36 | 161 |
| 5.5 | 5 | 1050 | aerogel | 508 | 0.3 | 68 |
| 5.5 | 5 | 1050 | xerogel | 521 | 0.28 | 105 |
| 5.5 | 20 | 800 | aerogel | 517 | 0.24 | 86 |
| 5.5 | 20 | 800 | xerogel | 493 | 0.26 | 63 |
| 5.5 | 20 | 1050 | aerogel | 474 | 0.23 | 59 |
| 5.5 | 20 | 1050 | xerogel | 460 | 0.25 | 74 |
| 7.0 | 5 | 800 | aerogel | 900 | 0.92 | 179 |
| 7.0 | 5 | 800 | xerogel | 591 | 0.20 | 113 |
| 7.0 | 5 | 1050 | aerogel | 753 | 1.32 | 142 |
| 7.0 | 5 | 1050 | xerogel | 540 | 0.40 | 106 |
| 7.0 | 20 | 800 | aerogel | 929 | 1.31 | 146 |
| 7.0 | 20 | 800 | xerogel | 586 | 0.44 | 124 |
| 7.0 | 20 | 1050 | aerogel | 804 | 1.42 | 144 |
| 7.0 | 20 | 1050 | xerogel | 515 | 0.44 | 104 |
| average = | | | | 607.6 | 0.543 | 112.6 |
| standard deviation = | | | | 151.5 | 0.434 | 36.3 |

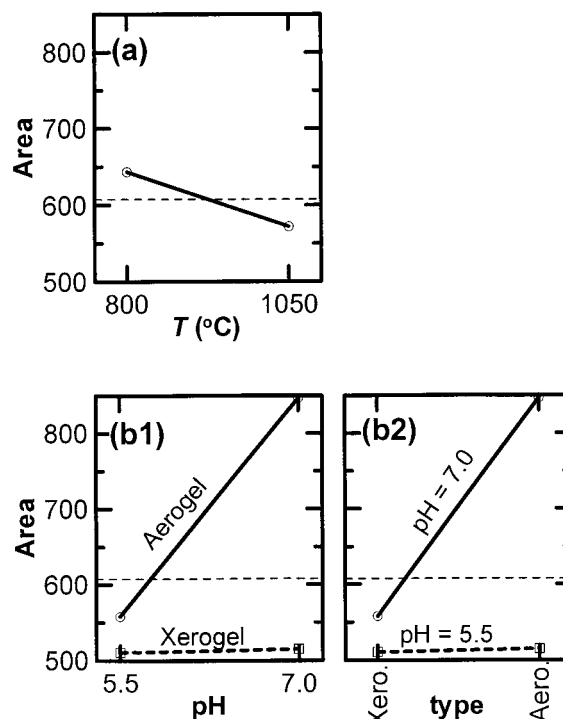
Table 3. Response Variables from the Carbon Aerogel Full 2³ Factorial Design

| initial solution pH | solids content (wt %) | pyrolysis temperature (°C) | surface area (m ² /g) | pore volume (cm ³ /g) | electrochemical capacitance (F/g) |
|----------------------|-----------------------|----------------------------|----------------------------------|----------------------------------|-----------------------------------|
| 5.5 | 5 | 800 | 561 | 0.32 | 128 |
| 5.5 | 5 | 1050 | 508 | 0.30 | 68 |
| 5.5 | 20 | 800 | 517 | 0.24 | 86 |
| 5.5 | 20 | 1050 | 474 | 0.23 | 59 |
| 7.0 | 5 | 800 | 900 | 0.92 | 179 |
| 7.0 | 5 | 1050 | 753 | 1.32 | 142 |
| 7.0 | 20 | 800 | 929 | 1.31 | 146 |
| 7.0 | 20 | 1050 | 804 | 1.42 | 144 |
| average = | | | 680.8 | 0.758 | 119.0 |
| standard deviation = | | | 186.6 | 0.539 | 42.9 |

Table 4. Response Variables from the Carbon Xerogel Full 2³ Factorial Design

| initial solution pH | solids content (wt %) | pyrolysis temperature (°C) | surface area (m ² /g) | pore volume (cm ³ /g) | electrochemical capacitance (F/g) |
|----------------------|-----------------------|----------------------------|----------------------------------|----------------------------------|-----------------------------------|
| 5.5 | 5 | 800 | 569 | 0.36 | 161 |
| 5.5 | 5 | 1050 | 521 | 0.28 | 105 |
| 5.5 | 20 | 800 | 493 | 0.26 | 63 |
| 5.5 | 20 | 1050 | 460 | 0.25 | 74 |
| 7.0 | 5 | 800 | 591 | 0.20 | 113 |
| 7.0 | 5 | 1050 | 540 | 0.40 | 106 |
| 7.0 | 20 | 800 | 586 | 0.44 | 124 |
| 7.0 | 20 | 1050 | 515 | 0.44 | 104 |
| average = | | | 534.4 | 0.329 | 106.3 |
| standard deviation = | | | 46.1 | 0.093 | 29.9 |

four factors and all of their possible interactions with each other, where A, B, C, and D correspond to gel pH, weight percentage of solids, pyrolysis temperature, and gel type, respectively. In other words, the main effects of A, B, C, and D, the two-factor interaction effects of AB, AC, AD, BC, BD, and CD, the three-factor interaction effects of ABC, ABD, BCD, and ACD, and the four-factor interaction effect of ABCD are all taken into account in this plot. Figure 1a indicates that, within a confidence level of 90%, the only combinations that significantly affect the surface area are, in order of significance, the gel pH, gel type, gel pH–gel type interaction, and pyrolysis temperature, as indicated from the relative lengths of the corresponding bars. Figure 1b, which further substantiates these results, is interpreted as follows. Ideally, if the factors and their interactions have no effect at all on the response variable, a vertical line passing through the zero of the abscissa would be the result. According to the theory behind a probability plot, however, any points that tend to form a straight line that might be slightly sloped about the zero of the abscissa and generally passing through the zero of the ordinate suggests that the factors and their interactions corresponding to these points also have essentially no effect on the response variable. The points that do not fall on the straight line shown in Figure 1b correspond to the gel pH, pyrolysis temperature, gel type, and gel pH–gel type two-factor interaction, which indicates that these are the only factors and factor interactions that have a significant effect. However, once a factor interaction has been identified as being significant, it is no longer meaningful to look at the individual factors involved; rather, only the interaction is considered, because the response to one factor depends on the level or levels of the other factor or factors involved. Therefore, it is appropriate to study only the effects of the pyrolysis temperature and the two-factor interaction between the gel pH and

**Figure 2.** Significant effects of (a) pyrolysis temperature and (b) gel pH–gel type interaction on the surface area of the carbon gels.

gel type. The effects of these variables on the surface area are shown in Figure 2.

Figure 2a indicates that the pyrolysis temperature has a negative effect on the total surface area, i.e., an increase in the pyrolysis temperature produces a carbon gel with a lower surface area. This result is in agreement with the results found by Lin and Ritter¹⁴ under similar conditions but only for carbon xerogels. The factor interaction plot, shown in Figure 2b1 and 2b2, equivalently reveals many interesting features of the effects of the gel pH–gel type interaction on the surface area. For example, Figure 2b1 shows that, in going from the low to the high gel pH, the effect is much more pronounced on the carbon aerogels than on the carbon xerogels. In other words, the surface area of the carbon xerogel is relatively insensitive to a change in the gel pH. In contrast, the surface area nearly doubles for the carbon aerogel in going from the low to the high pH setting. However, increasing the gel pH results in higher surface areas for both the carbon aerogels and xerogels, but only very slightly so for the carbon xerogels. This result indicates the importance of controlling the initial solution (gel) pH during synthesis, especially in the case of carbon aerogels. Another way of interpreting this interaction plot is to examine the change in surface area in going from the carbon xerogel to the carbon aerogel at constant gel pH, as shown in Figure 2b2. At the lower pH setting, the surface areas of the two carbon gels are very similar, whereas at the higher pH setting, the surface area of the carbon aerogel is much higher than that of the carbon xerogel. This interpretation leads to the same conclusions, however.

To explore these effects further, the gel pH–gel type interaction is analyzed through two 2³ factorial designs, one for the carbon aerogels and one for the carbon xerogels. In these designs, the effects of the gel pH, weight percentage of solids, and pyrolysis temperature are compared in Figures 3–6. Figure 3 shows the Pareto and normal probability plots for the effects of the seven

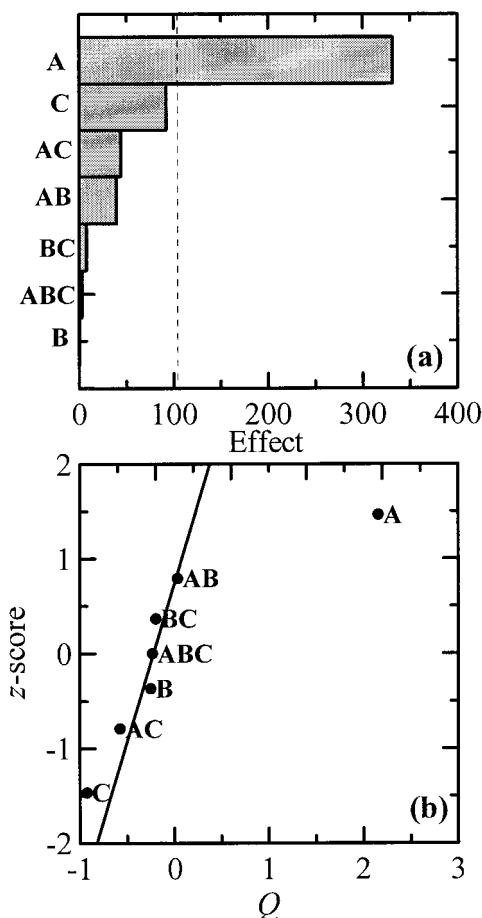


Figure 3. (a) Pareto and (b) normal probability plots for the effects of (A) gel pH, (B) weight percentage of solids, and (C) pyrolysis temperature on the surface area of the carbon aerogels. The vertical line in the Pareto plot indicates a confidence limit of 90% ($\alpha = 0.10$).

possible factors and factor combinations (A, B, C, AB, AC, BC, and ABC) on the surface area of the carbon aerogels. Clearly, the gel pH has the most significant effect within the 90% confidence limit. However, the pyrolysis temperature is also significant with respect to the other combinations. A comparison of the magnitudes of the effects of these two factors is shown in Figure 4. The effect of the gel pH (shown in Figure 4b) is much more pronounced and positive compared to that of the pyrolysis temperature (shown in Figure 4a), which exhibits only a modest negative effect. In contrast, none of these variables has a significant effect on the surface area of the carbon xerogels within the 90% confidence level. Therefore, a confidence level of 50% is adopted; the resulting Pareto and normal probability plots are shown in Figure 5. In this case, the gel pH is still significant, but less so than the pyrolysis temperature, and the weight percentage of solids is the least significant. The magnitudes of the significances of these three factors on the surface area of the carbon xerogels are illustrated in Figure 6. The pyrolysis temperature, gel pH, and weight percentage of solids are almost equally significant, but exhibit different trends. The gel pH produces a positive effect on the surface area, whereas the pyrolysis temperature and weight percentage of solids cause negative effects. Nevertheless, the overall effects exhibited by the carbon xerogels (Figure 6) are almost negligible compared to those exhibited by the carbon aerogels (Figure 4).

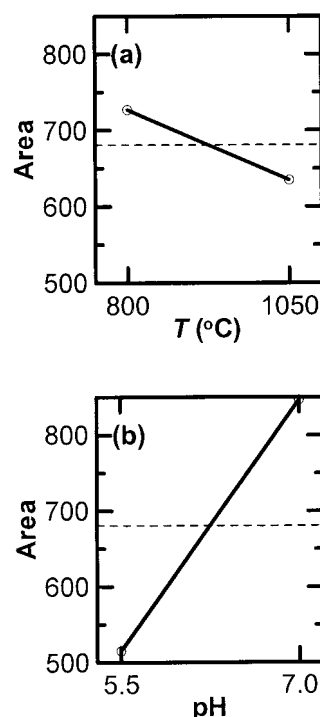


Figure 4. Significant effects of (a) pyrolysis temperature and (b) gel pH on the surface area of the carbon aerogels.

Figure 7 shows the Pareto and normal probability plots for pore volume. Only gel pH, gel type, and gel pH–gel type interaction have any significant effects. The weight percentage of solids and pyrolysis temperature do not significantly affect the pore volume within the range of the levels of the factors. Because of the interaction, as mentioned above, it is necessary to interpret only the interaction rather than the individual factors involved; Figure 8 shows the corresponding interaction plot. Clearly, the effect on the pore volume in going from the low to the high pH setting is much more pronounced for the carbon aerogel than for the carbon xerogel, as shown in Figure 8a1, similarly to the effect on surface area. Moreover, Figure 8a2 shows that the pore volumes of the two types of carbon gels are similar at the lower pH setting (dashed line), but not at the higher pH setting (solid line), where the pore volume of the carbon aerogel is markedly larger than that of the carbon xerogel, as shown in Figure 8a1. This is again similar to the effect on surface area. The similarity between the effects of the gel pH on the surface area and pore volume is not surprising because these properties tend to correlate with each other, as shown in Figure 9. This correlation, presented empirically in a reciprocal form, is implicit and deduced from the common dependences on the gel pH as the major contributor. Overall, these results suggest that the pore volume (akin to surface area) of the carbon aerogel is much more sensitive to slight changes in the initial solution (gel) pH during synthesis than the carbon xerogel.

Thus, it is also important to study the effects of these different factors on both the carbon aerogels and xerogels separately via the 2^3 factorial designs. Figure 10 shows the corresponding Pareto and normal probability plots of the effects of the different factors on the pore volume of the carbon aerogels. Figure 10a shows very clearly that only the gel pH exhibits a significant effect; the magnitude of this effect is shown in Figure 11, which

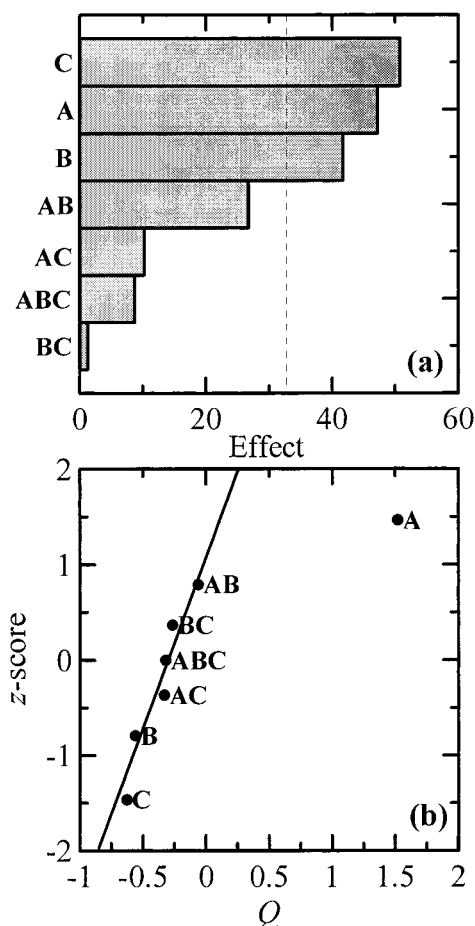


Figure 5. (a) Pareto and (b) normal probability plots for the effects of (A) gel pH, (B) weight percentage of solids, and (C) pyrolysis temperature on the surface area of the carbon xerogels. The vertical line in the Pareto plot indicates a confidence limit of 50% ($\alpha = 0.50$).

reveals it to be significant and positive. The effects of these variables on the pore volume of the carbon xerogels is shown in Figure 12. Note that, within the 90% confidence limit, no significant effect is observed for any of these variables; however, a confidence level of 50% reveals the most important variable to be the interaction between the gel pH and the weight percentage of solids. Figures 13a1 and 13a2 show the corresponding interaction plots. Figure 13a1 shows that, at the low pH setting, the weight percentage of solids has a negative effect on the pore volume of the carbon xerogel, whereas at the high gel pH, the effect of weight percentage of solids is more pronounced and positive. The other interpretation shown in Figure 13a2 reveals a very small negative effect of the pH setting at the low weight percentage of solids and a marked positive effect at the high weight percentage of solids.

The extreme importance of the gel pH in determining the surface areas and pore volumes of these carbon gels is believed to be due to the limited extent of reaction between resorcinol and formaldehyde to form individual, fairly small clusters at the higher pH setting (lower concentration of protons). Because the cross-linking of these clusters is believed to begin only after all of the resorcinol is reacted with formaldehyde through the condensation reaction, this increases the chances for the already-formed clusters to cross-link with each other and, in effect, form a more porous polymeric structure. Moreover, this trend is more sensible in the organic

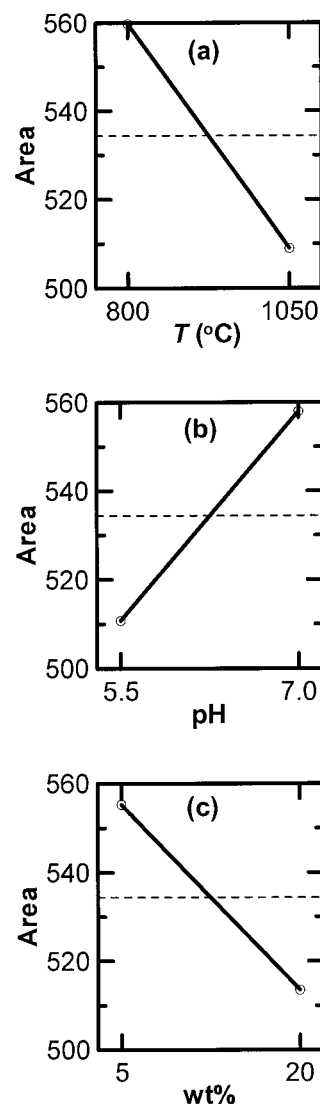


Figure 6. Significant effects of (a) pyrolysis temperature, (b) gel pH, and (c) weight percentage of solids on the surface area of the carbon xerogels.

aerogel than in the organic xerogel because the latter loses most of its pore structure through the evaporation of the solvent. The negative effect of the pyrolysis temperature on the surface area is in agreement with the results found by Lin and Ritter,¹⁴ which indicated a significant reduction of the micropores at high pyrolysis temperatures. A possible explanation for this trend is that the high temperatures result in carbonization rates that are too high and might cause the rupture of some of the walls between the adjacent micropores. A behavior such as this would decrease the surface area significantly. However, as also indicated by Lin and Ritter,¹⁴ this effect could be resolved after very long pyrolysis times. As expected from the high porosities of such polymeric structures, higher surface areas tend to correspond to higher pore volumes, as shown in Figure 9.

Electrochemical Double-Layer Capacitance Analysis. Figure 14 shows the Pareto and normal probability plot for the single-electrode electrochemical double-layer capacitance. This plot can be interpreted in two ways. First, because all of the data points tend to form a straight line in Figure 14b, it can be concluded that none of the factors and their interactions have any

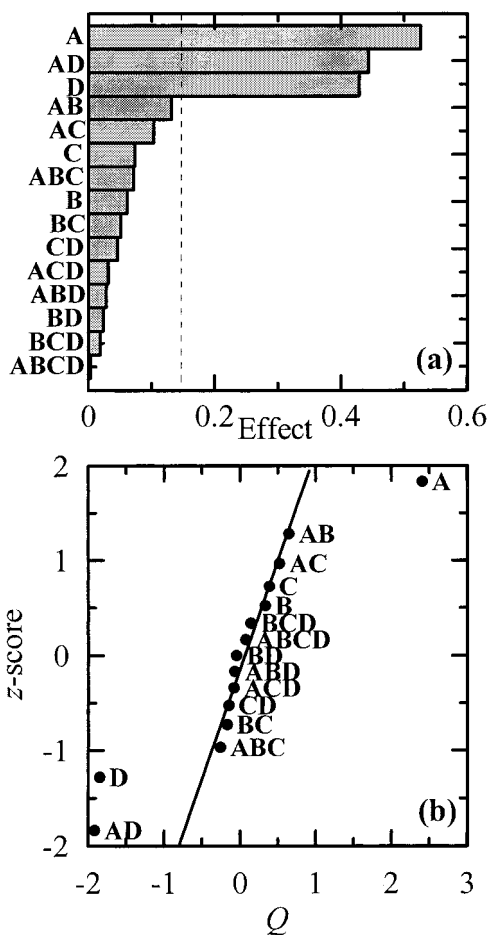


Figure 7. (a) Pareto and (b) normal probability plots for the effects of (A) gel pH, (B) weight percentage of solids, (C) pyrolysis temperature, and (D) gel type on the pore volume of the carbon gels. The vertical line in the Pareto plot indicates a confidence limit of 90% ($\alpha = 0.10$).

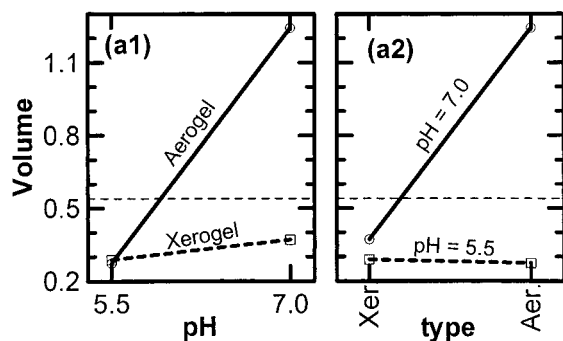


Figure 8. Significant effects of the gel pH–gel type interaction on the pore volume of the carbon gels.

effect on the capacitance. This result can also be indicated with the 90% confidence line, which falls at the limit of the longest bar in Figure 14a. However, a change in capacitance of about 20 F/g is considered to be significant. Therefore, the confidence level is lowered to 64% to include effects within this deviation. The results from the Pareto and normal probability plots indicate that gel pH, weight percentage of solids, and pyrolysis temperature as main effects and gel pH–gel type and gel pH–solids weight percent as two-factor-interaction effects all have significant effects on the capacitance. The main-effect and interaction plots for these combinations are shown in Figure 15. The pyrolysis temperature has a modest negative effect on the

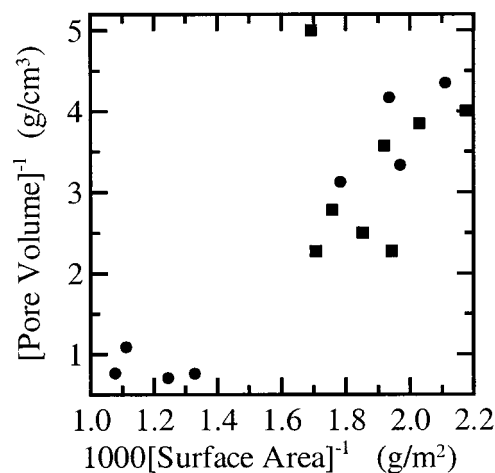


Figure 9. Implicit relationship between the surface area and pore volume of the carbon aerogels (circles) and xerogels (squares).

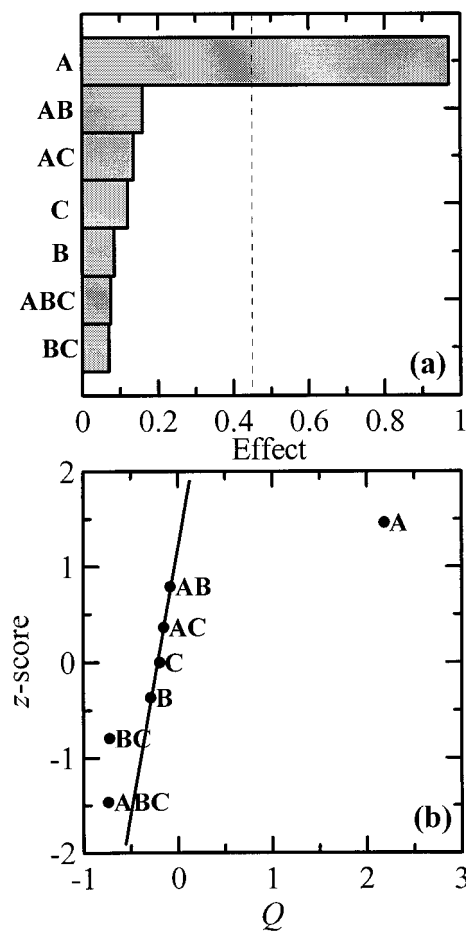


Figure 10. (a) Pareto and (b) normal probability plots for the effects of (A) gel pH, (B) weight percentage of solids, and (C) pyrolysis temperature on the pore volume of the carbon aerogels. The vertical line in the Pareto plot indicates a confidence limit of 90% ($\alpha = 0.10$).

capacitance (Figure 15a). Similar negative effects are realized at the high pH setting when comparing the carbon aerogel to the carbon xerogel, as shown in Figures 15b1 and 15b2, and at the low pH setting in going from the low to the high weight percentage of solids, as shown in Figures 15c1 and 15c2. Only a modest positive effect is observed at the low pH setting when going from carbon aerogels to xerogels in the gel pH–gel type interaction plot (Figure 15b) and a very

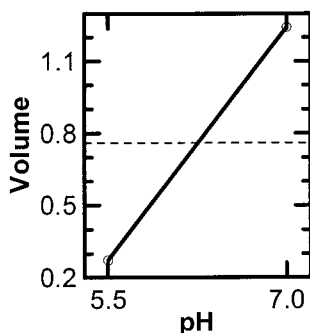


Figure 11. Significant effects of the gel pH on the pore volume of the carbon aerogels.

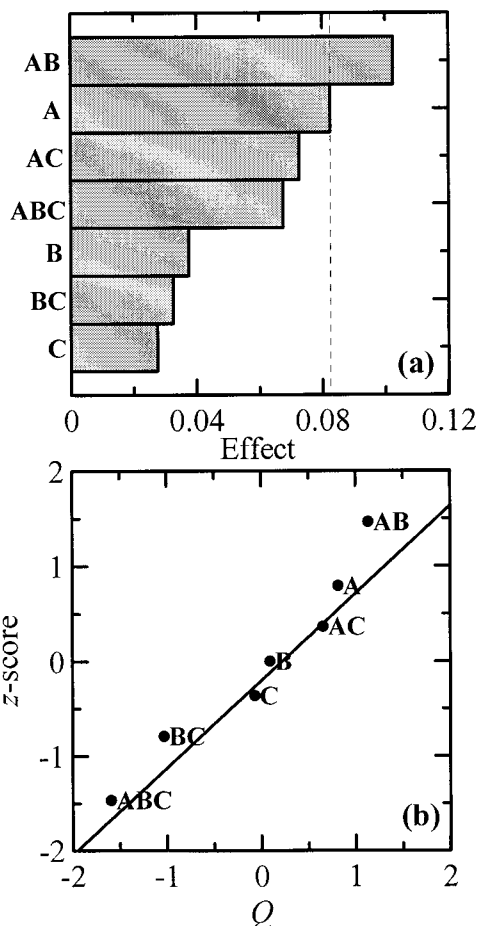


Figure 12. (a) Pareto and (b) normal probability plots for the effects of (A) gel pH, (B) weight percentage of solids, and (C) pyrolysis temperature on the pore volume of the carbon aerogels. The vertical line in the Pareto plot indicates a confidence limit of 50% ($\alpha = 0.50$).

small negative effect when increasing the weight percentage of solids at the high pH setting in the gel pH–solids weight percent interaction plot (Figure 15c). The alternative interpretation reveals significant positive effects of the pH setting for the carbon aerogel (Figure 15b1) and the high weight percentage of solids (Figure 15c1), with only minor effects realized at the opposing settings.

To separate the effects of these different factors from their interactions with the gel type, two 2^3 factorial designs were performed on the capacitance. Figure 16 shows the corresponding Pareto and normal probability plots for the carbon aerogels. The vertical line in Figure 16a represents the 53% confidence limit, which also

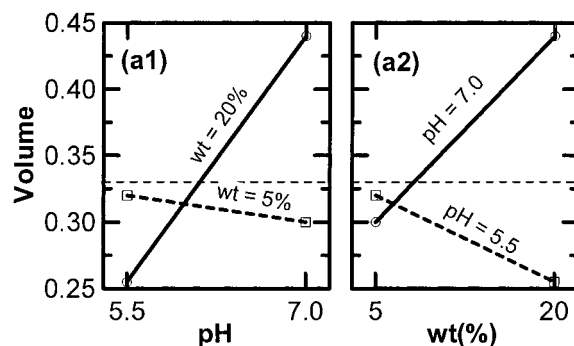


Figure 13. Significant effects of gel pH–solids weight percent interaction on the pore volume of the carbon xerogels.

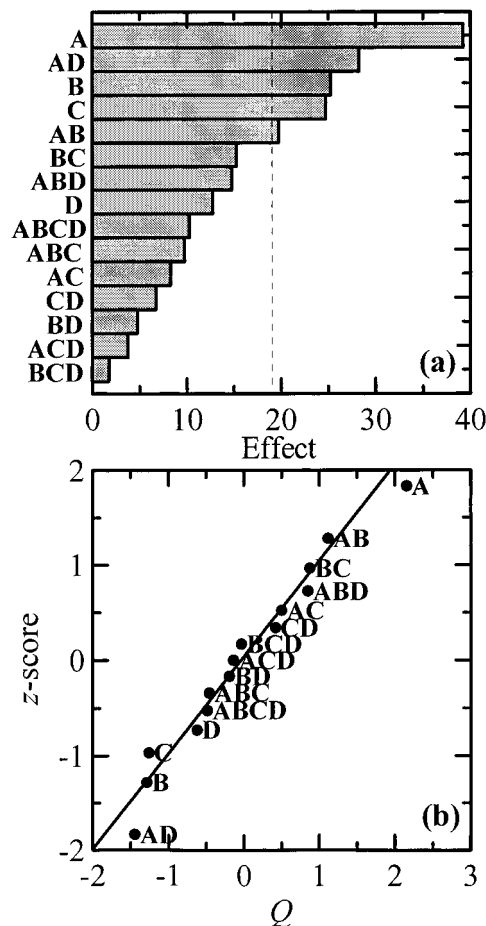


Figure 14. (a) Pareto and (b) normal probability plots for the effects of (A) gel pH, (B) weight percentage of solids, (C) pyrolysis temperature, and (D) gel type on the electrochemical double-layer capacitance of the carbon gels. The vertical line in the Pareto plot indicates a confidence limit of 64% ($\alpha = 0.36$).

corresponds to a minimum effect of ~ 20 F/g. As a result, the gel pH, pyrolysis temperature, and weight percentage of solids exhibit significant effects within this level of confidence. Note that the gel pH–solids weight percent interaction vanishes for the carbon aerogels. This suggests that the effect is due primarily from the response of the carbon xerogels to these factors as shown below. Figure 17 shows the main effects of these factors on the capacitance of the carbon aerogels. Figure 17b shows that the effect of the gel pH is marked and positive, whereas the effects of the pyrolysis temperature (Figure 17a) and weight percentage of solids (Figure 17c) are both only modest and negative, with

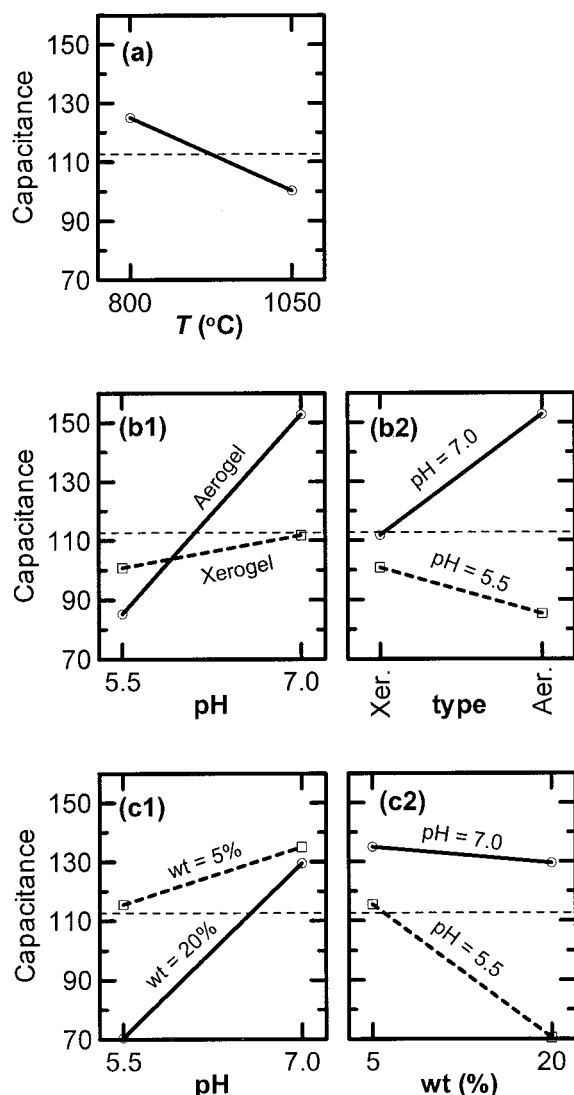


Figure 15. Significant effects of (a) pyrolysis temperature, (b) gel pH–gel type interactions, and (c) gel pH–solids weight percent interaction on the electrochemical double-layer capacitance of the carbon gels.

the weight percentage of solids exhibiting the least effect. Figure 18 shows the effects of these factors on the capacitance of the carbon xerogels. The most significant effects in this case result from the gel pH–solids weight percent interaction (as alluded to above), followed by the main effect of the weight percentage of solids. The interaction plot for the gel pH–solids weight percent interaction is shown in Figure 19. Figure 19a1 shows that the effect of the weight percentage of solids is marked and negative at the low pH setting; however, at the high pH setting, the effect diminishes and becomes relatively unimportant. Overall, Figure 19a2 (which is equivalent to 19a1) shows that the effect of initial solution (gel) pH is always significant and must be considered under different conditions. Figure 19a2 also reveals a modest negative effect of gel pH at the low solids weight percentage settings but a significant positive effect at the high solids weight percentage, with the effect vanishing at the point where the lines intersect in Figure 19a1 at some intermediate weight percentage of solids.

Overall, the effect of the gel pH tends to dominate the capacitance as it did the surface area and pore volume results. This result is not that surprising as the

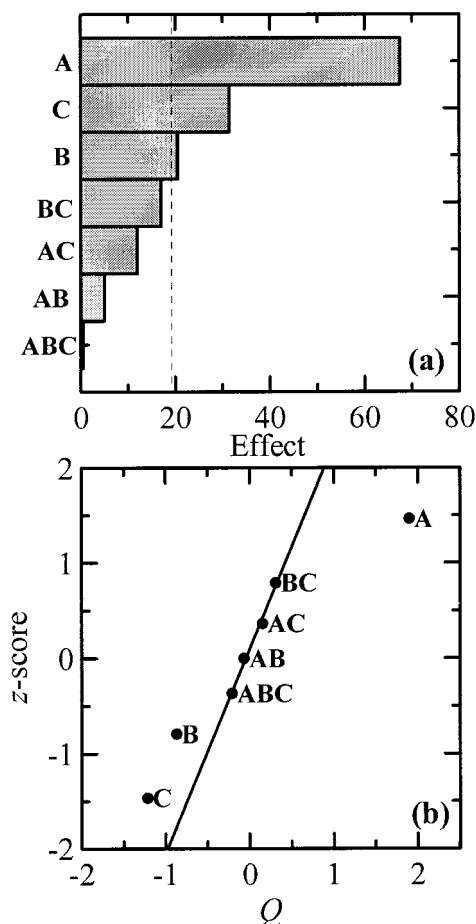


Figure 16. (a) Pareto and (b) normal probability plots for the effects of (A) gel pH, (B) weight percentage of solids, and (C) pyrolysis temperature on the electrochemical double-layer capacitance of the carbon aerogels. The vertical line in the Pareto plot indicates a confidence limit of 53% ($\alpha = 0.47$).

surface area and, to a lesser extent, the pore volume both tend to correlate with the capacitance. This implicit correlation, deduced again from the common dependences on the gel pH as the major contributor, is shown in Figure 20. The reciprocal capacitance tends to correlate quite well with the reciprocal surface area and also with the reciprocal pore volume, but less so. A close inspection of these results reveals a better and also broader correlation of the capacitance with the surface area of the carbon aerogels compared to that of the carbon xerogels. The same is true for the pore volume, but with a bit more scatter. These results agree well with those presented by Lin and Ritter¹⁴ for carbon xerogels.

Conclusions

Carbon aerogels and xerogels were synthesized via the sodium carbonate catalyzed sol–gel polycondensation of resorcinol with formaldehyde, followed by either supercritical or conventional drying and then carbonization under different conditions. A full 2^4 factorial design analysis was performed on 16 different materials to study the effect of the initial (gel) solution pH (5.5 and 7.0), solids content (5 and 20 wt %), pyrolysis temperature (800 and 1050 °C), and gel type (aerogel or xerogel) on the surface area, pore volume, and electrochemical double-layer capacitance. Also, two 2^3 factorial designs and analyses were done to reveal the effects of

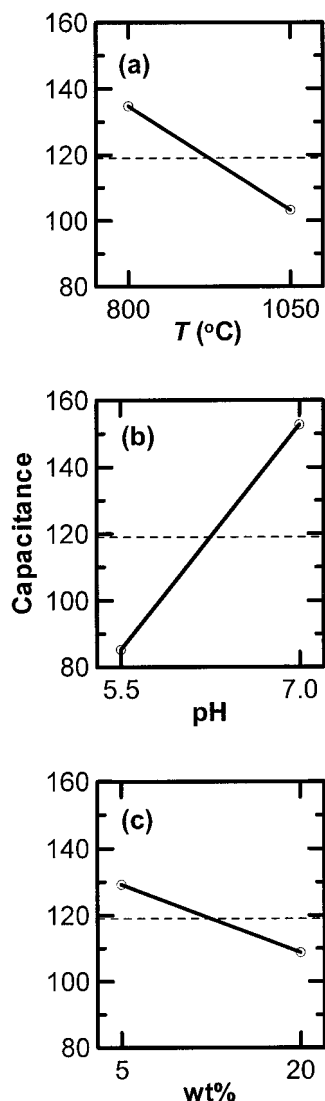


Figure 17. Significant effects of (a) pyrolysis temperature, (b) gel pH, and (c) weight percentage of solids on the electrochemical double-layer capacitance of the carbon aerogels.

the gel pH, weight percentage of solids, and pyrolysis temperature on the carbon aerogels and xerogels individually. Overall, significant differences between carbon aerogels and carbon xerogels were revealed through this design of experiments approach to materials synthesis. Specific factor interactions were easily observed that could not be readily resolved with the approach of changing one factor at a time. Moreover, the effects of each factor and any factor interactions that were revealed were unique to each response variable. The observed trends that could be used to obtain general guidelines that might be beneficial in tailoring these highly porous carbon materials for specific applications are summarized below.

The surface area of the carbon gels, in general, increased with a decrease in pyrolysis temperature and an increase in gel pH. An increase in the weight percentage of solids caused the surface area of the carbon xerogels to decrease but had no significant effect on the surface area of the carbon aerogels. The pore volume of the carbon gels, in general, also increased with an increase in gel pH; however, the pyrolysis temperature and weight percentage of solids exhibited no significant effects on the pore volume. This was also

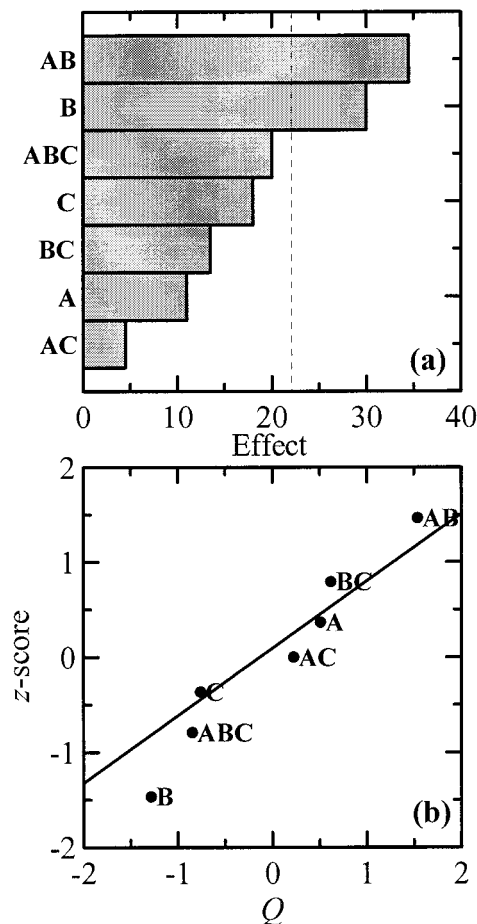


Figure 18. (a) Pareto and (b) normal probability plots for the effects of (A) gel pH, (B) weight percentage of solids, and (C) pyrolysis temperature on the electrochemical double-layer capacitance of the carbon xerogels. The vertical line in the Pareto plot indicates a confidence limit of 50% ($\alpha = 0.50$).

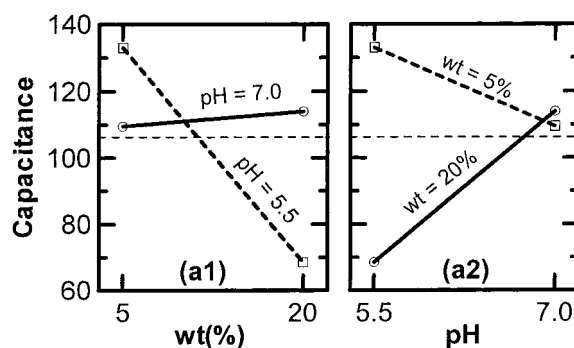


Figure 19. Significant effects of gel pH–solids weight percent interaction on the pore volume of the carbon xerogels.

the case for the carbon aerogels alone. In contrast, the effect of the gel pH on the pore volume of the carbon xerogels depended on the solids weight percentage. In other words, a factor interaction between the gel pH and weight percentage of solids was observed. At low weight percentage of solids, the pore volume increased only slightly with a decrease in gel pH; at high weight percentage of solids, the pore volume increased markedly, but with an increase in the gel pH. The electrochemical double-layer capacitance of the carbon gels increased with an increase in gel pH, decrease in weight percentage of solids, and decrease in pyrolysis temperature, but the gel pH had the greatest effect. This was also true for the carbon aerogels alone. There was no

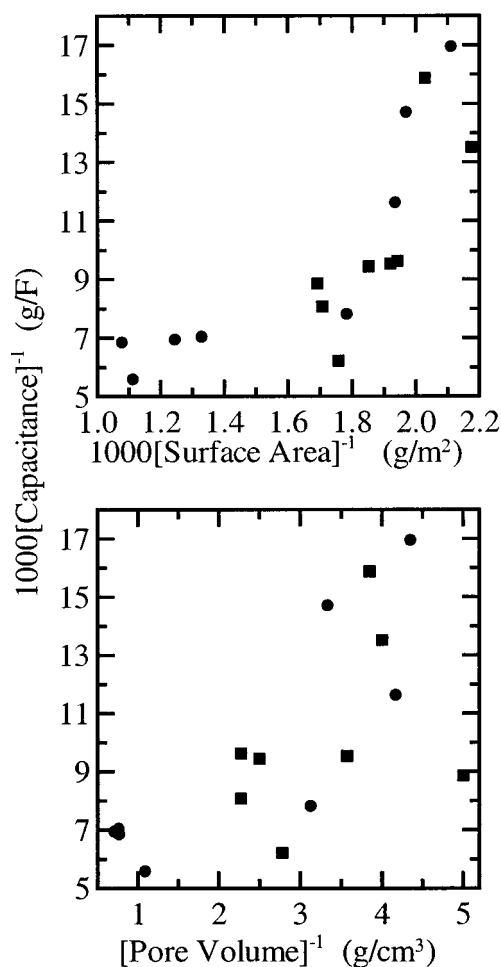


Figure 20. Implicit relationship between the surface area and pore volume of the carbon aerogels (circles) and xerogels (squares).

significant effect of the pyrolysis temperature on the capacitance of the carbon xerogels; however, the effect of the gel pH depended on the weight percentage of solids, revealing a factor interaction. At the low solids weight percentage, the capacitance increased marginally with a decrease in gel pH, and at the high solids weight percentage, it decreased significantly. It is interesting to note that this same factor interaction was observed in the full 2^4 carbon gel factorial design; however, judging from the full 2^3 carbon aerogel and xerogel individual factorial designs, it became clear that the interaction was caused almost exclusively by the response of the carbon xerogels.

On average, the carbon aerogels exhibited higher surface areas, pore volumes, and capacitances than the carbon xerogels. Also, in general, higher surface areas correlated with higher pore volumes, and higher capacitances correlated with higher surface areas and also with higher pore volumes, but not as closely. The highest surface area (929 m²/g) was exhibited by a carbon aerogel synthesized with a high gel pH and high weight percentage of solids and pyrolyzed at low temperature. The highest pore volume (1.42 cm³/g) was exhibited by a different carbon aerogel obtained with the high factor settings. The highest capacitance (179 F/g) was exhibited again by a different carbon aerogel synthesized with a high gel pH and low weight percentage of solids and pyrolyzed at low temperature. The corresponding values of the response variables were much lower for the carbon xerogels and were obtained

under completely different conditions. The highest carbon xerogel surface area was 591 m²/g and was obtained at the high gel pH, low weight percentage of solids, and low pyrolysis temperature settings. The highest carbon xerogel pore volume was 0.44 cm³/g and was obtained with the high gel pH, high weight percentage of solids, and either pyrolysis temperature. The highest carbon xerogel capacitance was 161 F/g and was obtained at the low gel pH and low solids weight percentage factor settings. In general, the properties of the carbon aerogels were more sensitive to the synthesis and processing conditions than the carbon xerogels. This indicates that carbon aerogels might be more tunable to a specific application, but that the synthesis and processing conditions must be tightly controlled. Clearly, the opposite would be true for the carbon xerogels.

Acknowledgment

This material is based on work supported in part by the U.S. Army Research Office under Grant DAAH04-96-1-0421 and in part by the U.S. National Science Foundation under Grant GER-9554556.

Literature Cited

- (1) Pekala, R. W. Organic Aerogels From the Polycondensation of Resorcinol with Formaldehyde. *J. Mater. Sci.* **1989**, *24*, 3221.
- (2) Ruben, G. C.; Pekala, R. W.; Tillotson, T. M.; Hrubesh, L. W. Imaging Aerogels at the Molecular Level. *J. Mater. Sci.* **1992**, *27*, 4341.
- (3) Pekala, R. W.; Alviso, C. T.; Lemay, J. D. *Chemical Processing of Advanced Materials*; Hench, L. L., West, F. K., Eds.; John Wiley & Sons: New York, 1992.
- (4) Mayer, S. T.; Pekala, R. W.; Kaschmitter, J. L. The Aerocapacitor—An Electrochemical Double-Layer Energy-Storage Device. *J. Electrochem. Soc.* **1993**, *140*, 446.
- (5) Pekala, R. W.; Mayer, S. T.; Daschmitter, J. L.; Kong, F. M. *Sol-Gel Processing and Applications*; Plenum Press: New York, 1994; p 369.
- (6) Farmer, J. C.; Fix, D. V.; Mack, G. V.; Pekala, R. W.; Poco, J. F. Capacitive deionization of NH₄ClO₄ solutions with carbon aerogel electrodes. *J. Appl. Electrochem.* **1996**, *26*, 1007.
- (7) Miller, J. M.; Dunn, B.; Tran, T. D.; Pekala, R. W. Deposition of ruthenium nanoparticles on carbon aerogels for high energy density supercapacitor electrodes. *J. Electrochem. Soc.* **1997**, *144*, L309.
- (8) Tamon, H.; Ishizaka, H.; Mikami, M.; Okazaki, M. Porous structure of organic and carbon aerogels synthesized by sol-gel polycondensation of resorcinol with formaldehyde. *Carbon* **1997**, *35*, 791.
- (9) Tamon, H.; Ishizaka, H. Porous characterization of carbon aerogels. *Carbon* **1998**, *36*, 1397.
- (10) Tamon, H.; Ishizaka, H.; Araki, T.; Okazaki, M. Control of mesoporous structure of organic and carbon aerogels. *Carbon* **1998**, *36*, 1257.
- (11) Reichenauer, G.; Emmerling, A.; Fricke, J.; Pekala, R. W. Microporosity in carbon aerogels. *J. Non-Cryst. Solids* **1998**, *225*, 210.
- (12) Lin, C.; Ritter, J. A. Effect of synthesis pH on the structure of carbon xerogels. *Carbon* **1997**, *35*, 1271.
- (13) Lin, C.; Ritter, J. A. Carbonization and activation of sol-gel derived carbon xerogels. *Carbon* **2000**, *38*, 849–861.
- (14) Lin, C.; Ritter, J. A.; Popov, B. N. Correlation of double-layer capacitance with the pore structure of sol-gel derived carbon xerogels. *J. Electrochem. Soc.* **1999**, *146*, 3639.
- (15) Brinker, C. J.; Scherer, G. W. *Sol-Gel Science*; Academic Press: San Diego, CA, 1990.
- (16) Farmer, J. C.; Bahowick, S. M.; Harrar, J. E.; Fix, D. V.; Martinelli, R. E.; Vu, A. K.; Carroll, K. L. Electrosorption of chromium ions on carbon aerogel electrodes as a means of remediating ground water. *Energy Fuels* **1997**, *11*, 337.
- (17) Saliger, R.; Fischer, U.; Herta, C.; Fricke, J. High surface area carbon aerogels for supercapacitors. *J. Non-Cryst. Solids* **1998**, *225*, 81–85.

(18) Glora, M.; Wiener, M.; Petričević, R.; Pröbstle, H.; Fricke, J. Integration of Carbon Aerogels in PEM Fuel Cells. *J. Non-Cryst. Solids* **2001**, *285*, 283.

(19) *Instruction Manual for Pulse Chemisor-2700*; Micromeritics Instrument Corporation: Norcross, GA, 1986.

(20) Xing, W.; Xue, J. S.; Zheng, T.; Gibaud, A.; Dahn, J. R. Correlation between Lithium Intercalation Capacity and Microstructure in Hard Carbons. *J. Electrochem. Soc.* **1996**, *143*, 3482–3491.

(21) Lochner, R. H.; Matar, J. E. *Designing for Quality*; ASQC Quality Press: Milwaukee, WI, 1990.

Received for review January 15, 2002

Revised manuscript received April 18, 2002

Accepted April 24, 2002

IE020048G